Indoles from the commensal microbiota act via the AHR and IL-10 to tune the cellular composition of the colonic epithelium during aging

Domonica N. Powell[a,b], Alyson Swimm[b], Robert Sonowal[b], Alexis Bretin[c], Andrew T. Gewirtz[c], Rheinallt M. Jones[d], and Daniel Kalman[b,1]

[a]Immunology and Molecular Pathogenesis Graduate Program, Emory University School of Medicine, Atlanta, GA 30322; [b]Department of Pathology and Laboratory Medicine, Emory University School of Medicine, Atlanta, GA 30322; [c]Institute for Biomedical Sciences, Center for Inflammation, Immunity, and Infection, Georgia State University, Atlanta, GA 30303; and [d]Division of Gastroenterology, Hepatology, and Nutrition, Department of Pediatrics, Emory University School of Medicine, Atlanta, GA 30322

Edited by Frederick M. Ausubel, Massachusetts General Hospital, Boston, MA, and approved July 13, 2020 (received for review February 18, 2020)

The intestinal epithelium is a highly dynamic structure that rejuvenates in response to acute stressors and can undergo alterations in cellular composition as animals age. The microbiota, acting via secreted factors related to indole, appear to regulate the sensitivity of the epithelium to stressors and promote epithelial repair via IL-22 and type I IFN signaling. As animals age, the cellular composition of the intestinal epithelium changes, resulting in a decreased proportion of goblet cells in the colon. We show that colonization of young or geriatric mice with bacteria that secrete indoles and various derivatives or administration of the indole derivative indole-3 aldehyde increases proliferation of epithelial cells and promotes goblet cell differentiation, reversing an effect of aging. To induce goblet cell differentiation, indole acts via the xenobiotic aryl hydrocarbon receptor to increase expression of the cytokine IL-10. However, the effects of indoles on goblet cells do not depend on type I IFN or on IL-22 signaling, pathways responsible for protection against acute stressors. Thus, indoles derived from the commensal microbiota regulate intestinal homeostasis, especially during aging, via mechanisms distinct from those used during responses to acute stressors. Indoles may have utility as an intervention to limit the decline of barrier integrity and the resulting systemic inflammation that occurs with aging.

aging | intestinal homeostasis | goblet cell | mucus

Aging is associated with an increase in baseline inflammation, a concept known as inflammaging, that is thought to contribute to frailty in geriatric populations (1, 2). One proposed mechanism for inflammaging is that a decline in epithelial barrier function allows for a leak of antigens that results in a chronic inflammatory response (3, 4). The colonic epithelium functions as a dynamic barrier that precludes systemic access of microbial and food-derived antigens while mediating cross-talk between the intestinal microbiota and the host (5). To maintain homeostasis, intestinal stem cells at the base of crypts proliferate and subsequently differentiate as they migrate toward the luminal surface. Daughter cells become either absorptive colonocytes or secretory cells, including goblet and neuroendocrine cells (6).

Goblet cells play a critical role in maintaining the integrity of the colonic barrier. Glycosylated mucin-2 (MUC2) proteins synthesized by goblet cells are released into the lumen, where they cross-link, expand, and undergo hydrolysis to form distinct layers over the colonic epithelium. The inner mucus layer is relatively impermeable to bacteria but porous enough to allow small molecules to reach the epithelial surface (7). The mucus also provides lubrication that limits the abrasive effects of fecal matter (8). When the mucus barrier is compromised, as in *Muc2*$^{-/-}$ mice, bacteria can interact directly with the epithelium, resulting in antigen and/or bacterial translocation into the lamina propria, which triggers an elevated inflammatory response (9, 10). Notably, goblet cells and colonic mucus have been associated with protection against various pathogens (11–13). Moreover, a reduction in goblet cells has been associated with colitis (14).

Whereas significant information is available about the intrinsic mechanisms that control stem cell proliferation and differentiation (6), much less is known about how these processes change during aging and how cell signaling pathways could be targeted to ameliorate the age-dependent decline in barrier function. Recent work by us and others has identified indole and its metabolites, including indole-3-carboxaldehyde (ICA), as molecules derived from commensal bacteria or from cruciferous vegetables (e.g., kale, broccoli and other *Brassica* varietals) that promote protection in response to damage by acute stressors including infection, irradiation, and hyperinflammatory allogeneic immune responses associated with graft-versus-host disease (GVHD) (15–17). In addition, indoles protect against a decline in health in aging mice when delivered over extended periods (weeks to months) in the absence of overt inflammatory stimuli (18).

The question arises as to how indoles orchestrate repair and immune responses so as to provide protection against diverse stressors. Indoles act via the aryl hydrocarbon receptor (AHR) to induce IL-22, which promotes stem cell-mediated repair of the epithelial barrier and protects against infection and damage caused by hyperinflammatory responses (15, 19–21). Likewise, indoles induce type I IFN signaling (17). However, induction of IL-22 and IFN signaling by indoles occurs only in the context of inflammatory responses to acute stressors. These responses appear

Significance

Aging is associated with an increase in baseline inflammation, called inflammaging, that may contribute to frailty in geriatric populations. Inflammaging could result from a decrease in anti-inflammatory mediators, such as IL-10, or a decrease in the capacity of the intestinal barrier to exclude inflammatory antigens. We show that during aging, mice lose goblet cells, which secrete mucus to protect the epithelium. Small molecules related to indole, which are secreted by the intestinal microbiota, act via the aryl hydrocarbon receptor and IL-10 to restore depleted goblet cell numbers in aged animals. Indoles may have utility as therapeutics to protect against or reverse changes in epithelial homeostasis associated with aging and may limit age-associated systemic inflammation, perhaps via induction of IL-10.

Author contributions: D.N.P., A.S., R.S., R.M.J., and D.K. designed research; D.N.P., A.S., R.S., and A.B. performed research; D.N.P., A.T.G., and D.K. analyzed data; and D.N.P. and D.K. wrote the paper.

The authors declare no competing interest.

This article is a PNAS Direct Submission.

[1]To whom correspondence may be addressed. Email: dkalman@emory.edu.

First published August 17, 2020.

to be temporally and spatially regulated. Thus, whereas IL-22 is only transiently induced in the colon, it is constitutively expressed in the small intestine and can be further induced by appropriate stimuli (22). Moreover, the effects of indoles appear to be context-dependent. IL-22 can induce proinflammatory or anti-inflammatory responses depending on the disease model (23). Taken together, these data led us to consider the possibility that the protective responses orchestrated by indoles in response to acute inflammatory stressors may be distinct from those induced during homeostasis, including during normal aging.

Here we show that indoles act via the AHR and IL-10 to alter intestinal homeostasis by augmenting intestinal cell turnover and promoting goblet cell differentiation, a process that becomes dysregulated as animals age. Our data raise the possibility of using indoles as therapeutic modalities to treat age-related infirmities associated with epithelial barrier disruption and systemic inflammation.

Results

ICA Increases Homeostatic Stem Cell Turnover in the Murine Colon. To assess the effects of exposure to indoles in the absence of stressors, we administered ICA or vehicle to young mice (age 8 to 12 wk) once daily for 2 wk by oral gavage. The proliferation of cells in the crypts was assessed, as measured by the ratio of Ki67 positivity to the total number of DAPI-positive nuclei per crypt (Fig. 1*D*). ICA did not change the number of DAPI-positive cells per crypt (Fig. 1 *A* and *B*) and did not cause substantial hyperplasia, as measured by crypt length, which increased only marginally (Fig. 1*C*). In vehicle-treated mice, Ki67-positive cells comprise on average one-third of the cells at the base of the crypt. With ICA, the Ki67-positive zone encompassed one-half of the crypt (Fig. 1 *A* and *D*). In accordance with these data, ICA also increased the number of cells staining positive for phosphohistone H3 (pHH3), a marker of cells transiting through G2 and M phases of the cell cycle (Fig. 1 *E* and *F*). Thus, protracted ICA treatment increased cell proliferation but not total cell number in the colonic crypts. Taken together, these data suggest that ICA induces a faster rate of turnover of cells in the crypt, although other, less likely possibilities exist.

Exposure to ICA Increases the Proportion of Goblet Cells in the Mouse Colon. To determine whether ICA alters the cellular composition of the crypts, histochemical or immunofluorescent staining was carried out on sections derived from young animals treated for 1 or 2 wk with ICA. Goblet cells were detected by staining with Alcian blue and periodic acid Schiff (AB-PAS), which recognizes glycosylated mucin (Fig. 1*G*), or by staining using an antibody against MUC2 (Fig. 1*H*). Whereas exposure to ICA for 1 wk did not produce significant changes in the number of goblet cells per crypt, exposure for 2 wk resulted in a robust increase ($P < 0.0001$; Fig. 1*I*). This increase represented an increased proportion of goblet cells per crypt (Fig. 1*J*), because no changes in total cell number were evident (Fig. 1*B*). In contrast, no change was evident in the number or proportion of enteroendocrine cells, detected by chromogranin A (CgA) staining (Fig. 1 *K* and *L*). This increased proportion of goblet cells persisted for at least 1 wk after ICA was removed (Fig. 1*M*). Taken together, these data indicate that protracted exposure to ICA induces a durable increase in the proportion of goblet cells in the colonic crypts.

Indoles Restore Depleted Goblet Cell Numbers in Geriatric Mice. To assess the effect of indoles on changes in intestinal homeostasis that occur during aging, geriatric C57BL/6 mice (age 22 to 24 mo) were administered vehicle or ICA for 2 wk. Histological assessment revealed lower goblet cell numbers per crypt in vehicle-treated geriatric mice compared with vehicle-treated young mice (Fig. 2*A*; compare squares in Fig. 2*B*). Accompanying this effect was a concomitant reduction in the thickness of the inner mucus layer (compare squares in Fig. 2*C*). When geriatric mice were treated with ICA for 2 wk, the number of goblet cells per crypt increased to a level comparable to that seen in young animals with or without ICA (Fig. 2 *A* and *B*), although no increase in mucus thickness was evident (Fig. 2*C*). Ki67 staining in geriatric animals appeared similar to that seen in young mice (compare Fig. 2*D* with Fig. 1*A* and Fig. 1*D* with Fig. 2*F*). ICA treatment increased proliferation, as measured by an increased proportion of Ki67-positive cells within crypts (Fig. 2 *D* and *F*). Although there was some variance in the values, the numbers of $DAPI^+$ cells per crypt appeared slightly decreased with ICA treatment; however, the numbers and variance were comparable to those from young animals (compare Figs. 2*D* and 1*B*), perhaps indicating a slight difference in turnover rate in geriatric animals. Thus, aging reduced the proportion of goblet cells within the crypt, and ICA treatment restored goblet cell numbers to a level comparable to that seen in young animals.

We next determined whether sustained colonization of the intestinal tract with commensal bacteria that produce indoles would also increase goblet cell numbers in geriatric mice. To do this, geriatric (2 y old) BALB/c mice were treated with streptomycin to reduce the number of commensal bacteria and then colonized with streptomycin-resistant strains of either *Escherichia coli* K12, which uses tryptophanase to convert tryptophan into indole and various indole derivatives including ICA, or, alternatively, *E. coli* K12Δ*tnaA*, a mutant strain lacking the bacterial tryptophanase gene that produces neither indole nor indole derivatives. On colonization, these strains reached levels of 10^8 CFU per gram of feces and composed the vast majority of culturable bacteria within the lumen. Animals remained colonized for up to 3 mo, the longest time tested. Finally, animals colonized with K12 expressed significantly higher levels of the indole metabolite indoxyl sulfate in the urine compared with animals colonized with K12Δ*tnaA*, verifying increased indole production by the intestinal microbiota in the K12-colonized mice (18). We had previously characterized this same group of animals and determined that ICA improved various measures of health, including motility, aggregate health scores, and weight, over a 3-mo period (18).

We compared goblet cell numbers in animals colonized for 3 mo with K12 and those colonized with K12Δ*tnaA* (Fig. 2*G*). Although there appeared to be a trend toward increases, the average number of goblet cells per crypt was quite variable (Fig. 2*H*), given the significant variation in crypt length in sections from different animals (Fig. 2*I*). When average numbers of goblet cells were normalized to average crypt length in the same animal (Fig. 2*J*), a highly significant increase in the proportion of goblet cells became apparent in animals colonized with K12 compared with those colonized with K12Δ*tnaA* (Fig. 2*J*). Taken together, these data demonstrate that the effect of indoles on goblet cell differentiation does not depend on the mouse strain, and that indoles either delivered exogenously or produced by the commensal microbiota can alter the cellular composition of the intestinal epithelium during aging.

Effects of ICA Depend on AHR but Not on IL-22 or Type 1 INFs. Indoles and related molecules, including ICA, are ligands for AHR (24). To determine whether the effects of ICA on cell proliferation and goblet cell differentiation depend on AHR, *Ahr*-deficient mice ($Ahr^{-/-}$) and wild-type (WT) littermates were treated with ICA for 2 wk. No significant increase in goblet cell numbers was detected in $Ahr^{-/-}$ mice compared with WT littermates (Fig. 3 *A* and *B*). Crypt length in $Ahr^{-/-}$ mice was not significantly different from that in WT mice and was unchanged following ICA treatment (Fig. 3*C*). In addition, no increase in cell proliferation was evident in $Ahr^{-/-}$ mice following ICA treatment (Fig. 3 *D* and *E*). Taken together, these data suggest that the effects of ICA on cell proliferation and goblet cell numbers depended upon AHR.

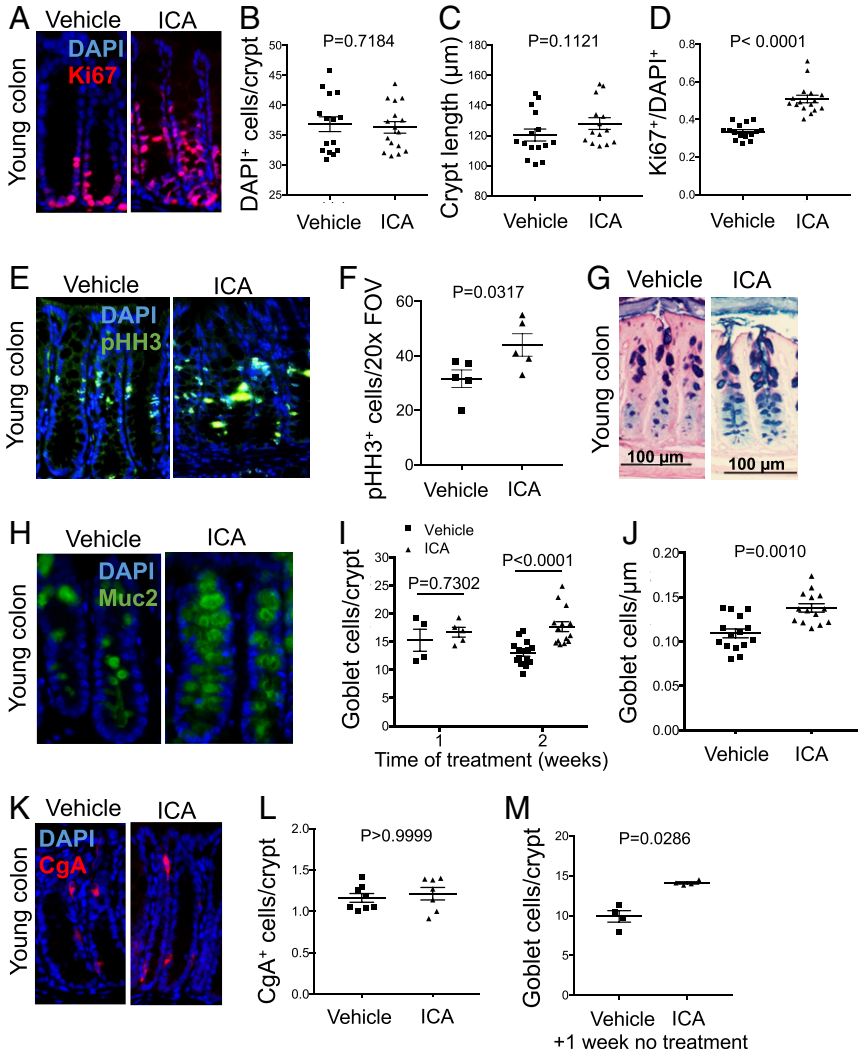

Fig. 1. ICA increases homeostatic stem cell turnover and goblet cell differentiation in the murine colon. Here 2- to 3-mo-old WT C57BL/6 mice were administered vehicle or 150 mg/kg ICA once daily for 1 or 2 wk as indicated (*A*–*L*) or for 2 wk with ICA followed by 1 wk without treatment (*M*). (*A*) Representative images of DAPI and Ki67 immunostaining of distal colon sections. (*B*) Quantitation of DAPI$^+$ cells per crypt. (*C*) Quantitation of average colon crypt length. (*D*) Quantitation of Ki67$^+$ cells per crypt normalized to the number of DAPI$^+$ cells per crypt. (*E*) Representative images of DAPI and pHH3 immunostaining of the distal colon. (*F*) Quantitation of pHH3$^+$ cells per field of view (FOV). (*G*) Representative images of AB-PAS staining of cells in distal colon. (*H*) Representative DAPI and MUC2 immunostaining of cells in distal colon. (*I*) Quantitation of AB-PAS$^+$ (goblet) cells per crypt following 1 or 2 wk of ICA treatment. (*J*) Quantitation of AB-PAS$^+$ (goblet) cells per crypt, normalized to crypt depth. (*K*) Representative chromogranin A (CgA) immunostaining (enteroendocrine cells) in distal colon. (*L*) Quantitation of CgA$^+$ cells per crypt. (*M*) Quantitation of AB-PAS$^+$ (goblet) cells in distal colon in animals treated with ICA for 2 wk followed by no treatment for 1 wk. Each point represents an individual mouse. Twenty full crypts per section and two sections per mouse were assessed for Ki67, AB-PAS, and CgA staining. Ten fields of view containing full crypts were assessed per section for pHH3. Data shown are representative of at least two independent experiments and are expressed as mean ± SEM. The Mann–Whitney *U* test was performed to calculate *P* values.

Activation of AHR in type 3 innate lymphoid cells by indoles induces transient expression of IL-22 in the context of various stressors (19, 22). We next determined the extent to which 2-wk treatment with ICA induced IL-22 levels in the colon and the small intestine in the absence of stressors. IL-22 was constitutively expressed in the small intestine of untreated mice; however, no detectable increase in IL-22 was evident following ICA treatment in either small intestine or colon, and IL-22 levels remained below the limit of detection in colons of untreated and ICA-treated animals alike (Fig. 3*F*). Furthermore, *Il22*-deficient mice (*Il22*$^{-/-}$) still showed an increase in goblet cell numbers after the 2-wk ICA treatment (Fig. 3 *G* and *H*). These data provide evidence that exposure to ICA over protracted periods and in the absence of stressors does not induce IL-22. These data further suggest that IL-22 does not contribute to the ICA-mediated increases in cell proliferation and the proportion of goblet cells.

Type I IFN also has been shown to mediate protective responses of ICA in response to radiation and inflammation associated with GVHD (17). To test whether the effects of ICA on goblet cells depend on type I IFN signaling, *Ifnar1*$^{-/-}$ mice, which lack the type I IFN receptor, were exposed to ICA for 2 wk. Goblet cell numbers in *Ifnar1*$^{-/-}$ mice increased to the same extent as in ICA-treated WT animals, suggesting that effects of ICA on goblet cells does not depend on type I IFN signaling (Fig. 3 *I* and *J*), in accordance with published data showing that indoles induce only a type I IFN response under acute stressor conditions (17).

Effects of ICA Are Mediated by IL-10. IL-10 has been implicated in regulating intestinal homeostasis (25, 26). To assess whether the effects of ICA on cell proliferation and goblet cell differentiation

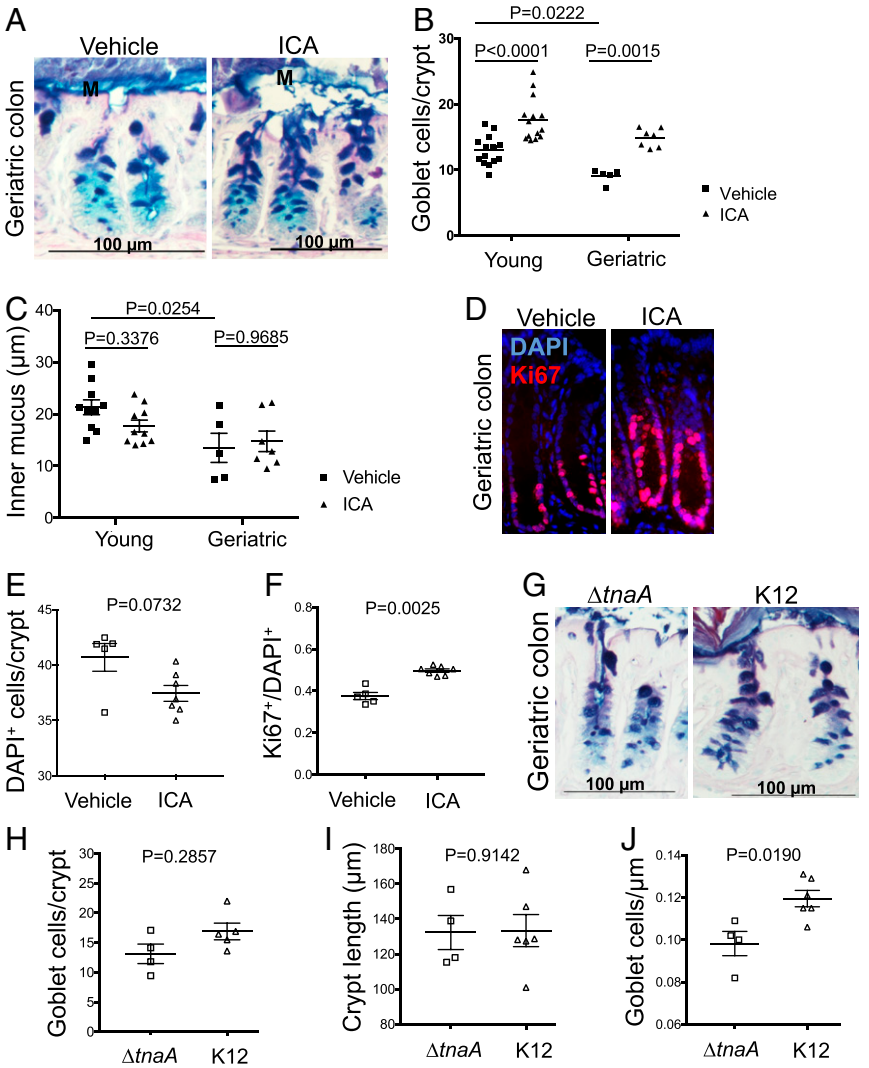

Fig. 2. ICA restores depleted goblet cell numbers in geriatric mice. (*A–F*) Geriatric (22 to 24 mo old) C57BL/6 mice were administered vehicle or 150 mg/kg ICA for 2 wk by oral gavage. (*A*) Representative images of AB-PAS staining (goblet cells) in distal colon of geriatric mice. "M" indicates the inner mucus layer. (*B*) Quantitation of AB-PAS staining (goblet cells) per crypt in young and geriatric mice. (*C*) Measurement of inner mucus layer thickness in young and geriatric mice. (*D*) Representative images of Ki67 immunostaining in distal colon of geriatric C57BL/6 mice. (*E*) Quantitation of $DAPI^+$ cells per crypt in geriatric C57BL/6 mice. (*F*) Quantitation of $Ki67^+$ cells per crypt normalized to $DAPI^+$ cells per crypt in geriatric C57BL/6J mice. (*G–J*) Geriatric 2-y-old BALB/c mice were treated with streptomycin and colonized with streptomycin and nalidixic acid-resistant K12 or K12Δ*tnaA* for 3 mo before histological assessment. (*G*) Representative AB-PAS staining (goblet cells) in distal colon of colonized geriatric BALB/c mice. (*H*) Quantitation of goblet cells per crypt in colonized geriatric BALB/c mice. (*I*) Average colon crypt length of geriatric BALB/c mice. (*J*) Goblet cell numbers per crypt normalized to crypt length of geriatric BALB/c mice. Ratios were computed by comparison of goblet cells to crypt length within the same mouse. Each dot represents an individual mouse. Twenty full crypts were counted per section. For mucus thickness, 10 measurements were made per section. Data are expressed as mean ± SEM. *P* values were calculated using two-way ANOVA with multiple comparisons (*B* and *C*) or the Mann–Whitney *U* test.

depend on IL-10, *Il10* transcript levels were measured by qPCR in young and geriatric animals. In response to ICA, *Il10* transcript levels increased in the colons of young mice by 2.5-fold on average (Fig. 4*A*). Differences in *Il10* transcript levels in geriatric mice were less robust, but one-half the ICA-treated animals expressed higher levels of *Il10* than were seen in all vehicle-treated animals (Fig. 4*B*). Although the increase did not reach the 0.05 level of significance, the probability of achieving the observed ordering of values was 0.17. In addition, no difference in *Il10* transcript levels was evident in colons of $Ahr^{-/-}$ mice (Fig. 4*C*).

To determine whether the effects of ICA on goblet cells depends on IL-10, young *Il10*-deficient ($Il10^{-/-}$) mice were treated with ICA for 2 wk. No increases in the numbers of $DAPI^+$ cells per crypt (Fig. 4*D*) or in crypt length (Fig. 4*E*) were evident after ICA treatment in $Il10^{-/-}$ mice. In contrast to WT animals, no increases in goblet cell numbers per crypt (Fig. 4 *E* and *F*), cell numbers per crypt, or cell proliferation (Fig. 4 *G–I*) were evident in $Il10^{-/-}$ animals. Taken together, these data suggest that the effects of treatment with ICA on cell proliferation and goblet cell differentiation depend on IL-10.

Discussion

The capacity of the intestine to regenerate via proliferation and differentiation of crypt stem cells remains vital for repairing damaged epithelia and facilitating antipathogen responses (27). Several lines of evidence indicate that indoles from the intestinal microbiota can alter responses to acute stressors (28). Indole derivatives such as ICA can induce IL-22 via AHR, which initiates an epithelial repair program (22). In addition, indoles induce type

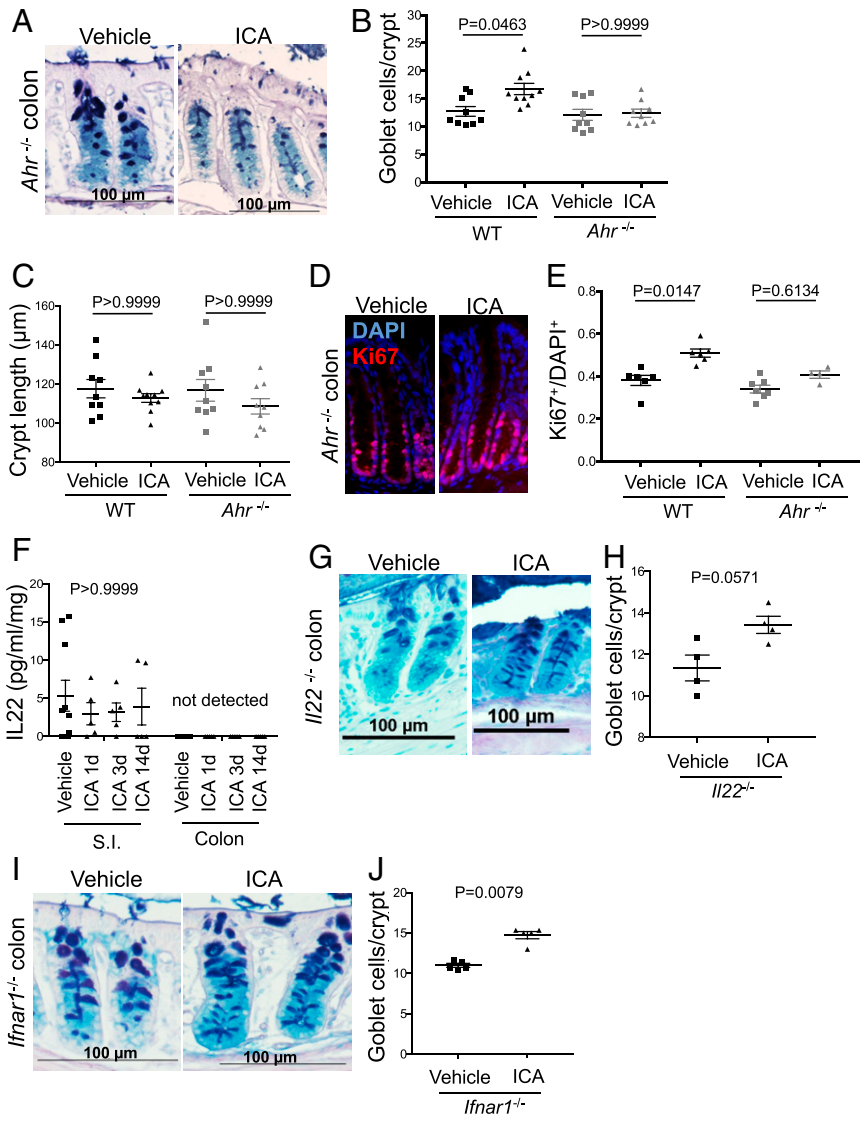

Fig. 3. Effects of ICA depend on AHR but not on IL-22 or type I IFN. (*A–E*) $Ahr^{-/-}$ mice and WT littermates were given vehicle or 150 mg/kg ICA for 2 wk. Data shown are pooled from two independent experiments. (*A*) Representative images of AB-PAS staining (goblet cells) in distal colon of $Ahr^{-/-}$ mice treated with vehicle or ICA for 2 wk. (*B*) Quantitation of goblet cells per crypt in $Ahr^{-/-}$ mice or WT littermates. (*C*) Average colon crypt length of WT and $Ahr^{-/-}$ mice. (*D*) Representative images of Ki67 immunostaining of distal colons of $Ahr^{-/-}$ mice. (*E*) Quantitation of $Ki67^{+}$ cells per crypt, normalized to $DAPI^{+}$ cells per crypt. (*F*) WT C56BL/6 mice received daily oral gavage with vehicle or 150 mg/kg ICA for 2 wk, then 2-cm pieces of distal colon or small intestine were excised and cultured ex vivo, and conditioned supernatant was collected for IL-22 ELISA. (*G–H*) $Il22^{-/-}$ mice received daily oral gavage with vehicle or 150 mg/kg ICA for 2 wk. (*G*) Representative images of AB-PAS staining (goblet cells) in distal colon of $Il22^{-/-}$ mice. (*H*) Quantitation of goblet cells per crypt. (*I* and *J*) $Ifnar1^{-/-}$ mice received daily oral gavage with vehicle or 150 mg/kg ICA for 2 wk. (*I*) Representative images of AB-PAS staining (goblet cells) in distal colon of $Ifnar1^{-/-}$ mice treated with vehicle or ICA. (*J*) Quantitation of goblet cells per crypt. Each dot represents an individual mouse. Twenty full crypts counted per section for AB-PAS staining. Data are expressed as mean ± SEM. *P* values were calculated using the Kruskal–Wallis test with Dunn's multiple comparisons (*B*, *C*, *E*, and *F*) or the Mann–Whitney *U* test (*H* and *J*).

I IFN in the context of radiation exposure and GVHD (17). However, the data presented here indicate that neither IL-22 nor type I IFN signaling functions in the context of homeostatic changes evident on protracted exposure to indoles (Fig. 3 *I* and *J*), raising the possibility that indoles regulate responses to stressors and homeostasis via distinct mechanisms (Fig. 4*J*). Here we show that protracted exposure to indoles alters the homeostatic setpoint within the crypts by increasing the proportion of goblet cells and promoting turnover of cells in the crypts (Fig. 1*I*). Moreover, we describe a mechanism whereby indoles regulate homeostasis, particularly as animals age, involving AHR and IL-10, a cytokine dispensable for acute infections (29). Our results are in accordance with a recent in vitro study in which the indole derivative indole-3-carbinol promoted goblet cell differentiation in enteroids via AHR (30).

It has been proposed that with age, the intestinal barrier becomes more permeable, and leakage of bacterial antigens from the lumen into the body cavity precipitates a systemic inflammatory response, a process known as inflammaging (3, 4, 31). However, evidence in support of inflammaging has remained somewhat limited. Diminishing numbers of goblet cells and thinning of the mucus layer during aging could lead to altered host-microbe relationships, increased exposure to circulating luminal antigens, and, consequently, increased inflammation (32, 33). In addition, reduced mucus production could contribute to constipation, a common complaint among the elderly (34), and permit abrasion by feces, leading to a

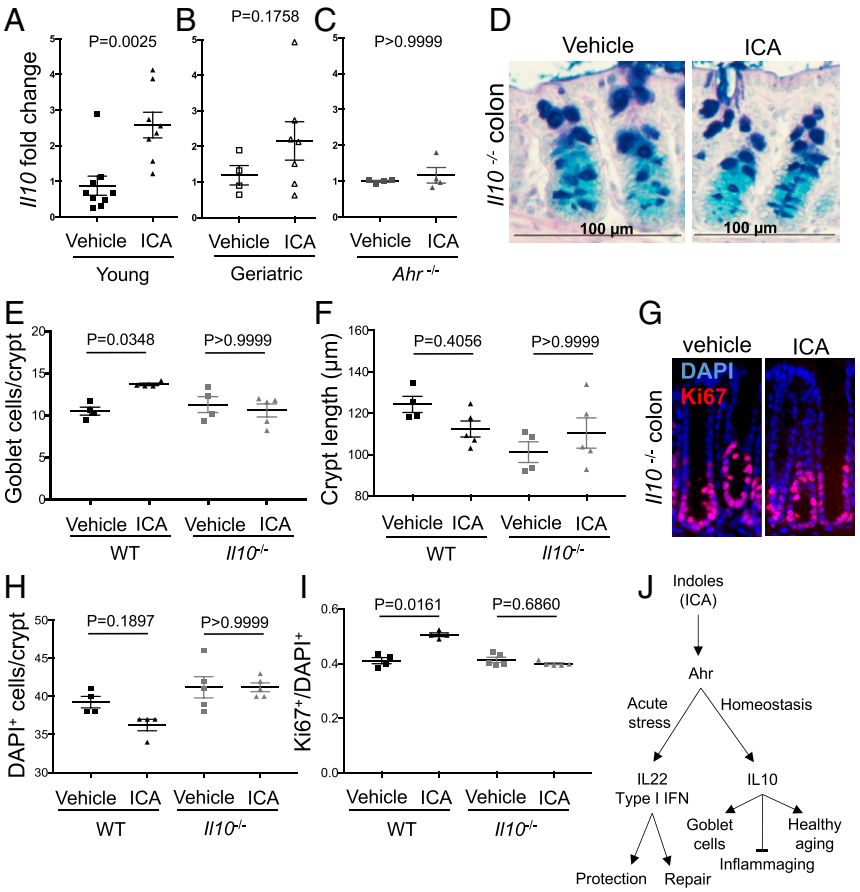

Fig. 4. Effects of ICA are mediated by AHR and IL-10. WT, *Il10*$^{-/-}$, and *Ahr*$^{-/-}$ mice were treated with vehicle 150 mg/kg ICA for 2 wk. (*A*–*C*) qPCR analysis of expression of *Il10* in colon tissue of young WT C56BL/6 mice (*A*), geriatric (22–24 mo old) WT C57BL/6 mice (*B*), or *Ahr*$^{-/-}$ (*C*) mice. (*D*–*I*) Measurement of goblet cells, proliferation, and cell numbers in *Il10*$^{-/-}$ mice and WT controls. (*D*) Representative images of AB-PAS stain (goblet cells) in distal colon of *Il10*$^{-/-}$ mice. (*E*) Quantitation of goblet cells per crypt in WT and *Il10*$^{-/-}$ animals. (*F*) Average colon crypt length in WT and *Il10*$^{-/-}$ animals. (*G*) Representative images of Ki67 immunostaining of distal colons of *Il10*$^{-/-}$ mice. (*H*) Quantitation of DAPI^{+} cells per crypt in WT and *Il10*$^{-/-}$ animals. (*I*) Quantitation of Ki67^{+} cells per crypt, normalized to DAPI^{+} cells per crypt in WT and *Il10*$^{-/-}$ animals. (*J*) Model of Indole effects during intestinal homeostasis and in response to acute stressors. Commensal-derived or exogenously supplied indoles, such as ICA, work through IL-22 and type I IFN to control protective responses to acute stressors or, alternatively, promote healthy aging and limit inflammaging via IL-10–mediated effects on goblet cell numbers and intestinal homeostasis. Each dot represents an individual mouse. Twenty full crypts were counted per section. Data are expressed as mean ± SEM. *P* values were calculated using the Mann–Whitney *U* test (*A* and *C*) or the Kruskal–Wallis test with multiple comparisons (*D*, *E*, *G*, and *H*).

damaged epithelial barrier and inflammation. Finally, while a decline in proliferation was not evident in geriatric mice, increased turnover associated with indoles could provide a significant benefit in the event of injury or infection.

Indoles and IL-10 likely influence multiple aspects of the intestinal barrier to protect against bacterial translocation and limit inflammatory responses under homeostatic conditions. In addition to increasing goblet cell numbers in geriatric animals (Fig. 2*B*), indoles also improve transepithelial resistance (17, 35) and regulate expression of the IL-10 receptor (IL-10R) on intestinal epithelial cells, perhaps as a means of further promoting IL-10 signaling (35). Taken together, these observations suggest that indoles can protect the epithelial barrier, especially during aging, and limit inflammation associated with transit of bacterial products.

We previously reported that colonization of geriatric mice with indole-producing bacteria for 3 mo augmented the lifespan and reduced frailty, including measures of overall health score, weight loss, and mobility, although the mechanistic basis for this protective effect was not elaborated (18). Here we demonstrate that in aged animals, reduced health scores are accompanied by loss of goblet cells in animals colonized with K12Δ*tnaA*, an effect reversed by colonization with K12 bacteria, which produce indoles (Fig. 2*B*). It is unlikely that goblet cells alone contribute to increased healthspan with indoles. However, our observation that indole can act via IL-10 (Fig. 4) may provide an important link. Future studies will be aimed at determining whether indole maintains intestinal homeostasis at youthful levels in older animals via IL-10. In this regard, increases in *Il10* transcript levels were evident in half of the geriatric animals tested (Fig. 4*B*). Such data did not appear to be random, as the Mann–Whitney *U* test indicated that the probability of such an ordering by of values by chance was 0.17. However, although the effect reached a significance level of 0.002 in younger animals, it did not reach the 0.05 level of significance in older animals, perhaps due to the increased variance evident in data from older animals (36, 37).

One interesting possibility is that activation of IL-10 by commensal microbiota can initiate protective reorganization of the epithelial barrier via up-regulation of goblet cells and other protective mechanisms while simultaneously limiting systemic inflammatory responses to bacterial antigens, supporting the idea that indoles are multifaceted microbiota-derived factors that limit inflammaging. In this regard, IL-10 is well recognized for its anti-inflammatory activity, and, importantly, levels of IL-10 decrease with age (38). Moreover, mice deficient in *Il10* exhibit increased inflammation throughout their lives and are increasingly susceptible to inflammatory conditions as they age, including

colitis (25, 39). Given the increased baseline inflammation, *Il10*$^{-/-}$ mice exhibit increased signs of frailty, including decreased mobility and early mortality, at younger ages than WT animals (40, 41), although the mismatch with WT animals in physiological and chronological age complicates a detailed comparison of these animals. Nevertheless, in a study of frail geriatric humans, the level of circulating bacterial muramyl dipeptide was inversely correlated with IL-10 level (42).

As noted above, IL-10 induced by indoles may protect against the onset of frailty during aging by limiting the decline in barrier function that permits translocation of bacterial products from the lumen into the lamina propria. In this regard, we have shown previously that ICA treatment of allogeneic bone marrow transplant recipients leads to reduced colonic inflammation, IL-6, and bacterial leakage into the mesenteric lymph nodes (17). ICA also induces protective systemic responses over longer periods. Thus, ICA increases survival of allo-BMT recipients even when discontinued and induces tolerance in allogeneic T cells (17). Whether such systemic effects depend on IL-10 is currently under investigation.

Because dysbiosis has been associated with deleterious changes with aging (2), our future studies will be aimed at measuring levels of indole or its derivatives in the colons of geriatric human subjects. In this context, indole levels may provide a predictive metric of health potential. In prospective bone marrow transplant recipients, indole levels predict susceptibility to intestinal GVHD and mortality (43), a metric that we plan to use to identify prospective patients for a clinical trial.

In conclusion, further delineation of the signaling pathways controlled by indoles, both within the intestinal epithelia and systemically, will facilitate the development of therapeutics that limit detrimental changes associated with aging or other inflammatory diseases and promote healthspan, the capacity to live better for longer.

Materials and Methods

Mice. C57BL/6J, B6.129P2-*Il10*^{tm1Cgn}/J (*Il10*$^{-/-}$), B6(Cg)-*Ifnar1*$^{tm1.2Ees}$/J (*Ifnar1*$^{-/-}$), and B6.129-*Ahr*^{tm1Bra}/J (*Ahr*$^{-/-}$) mice were purchased from The Jackson Laboratory or bred in-house at Emory University. Young male and female mice were used between 8 and 12 wk of age. Mice were allowed to acclimate in the facility for at least 1 wk following shipment. KO mice were housed separately from WT controls for at least 1 wk before and throughout the experiments. Treatment groups were also housed in separate cages. Geriatric male and female C57BL/6J mice were housed in our facility for 22 to 24 mo. Geriatric (2 y old) BALB/c mice were obtained from the Aged Rodent Colonies maintained by the National Institute on Aging, a division of the NIH. Animal handling and experimental protocols were in accordance with the *Guide for the Care and Use of Laboratory Animals* (44) and approved by Emory University's Institutional Animal Care and Use Committee. *Il22*$^{-/-}$ mice were bred and housed at Georgia State University under institutionally approved protocols (44).

ICA Administration. ICA (Sigma-Aldrich) was delivered daily for 14 d by oral gavage at a dose of 150 mg·kg^{-1}·d^{-1} in a vehicle of DMSO/PEG400/5% citric acid (1:4.5:4.5).

Colonization with K12 or K12Δ*tna*A. Geriatric (2 y old) BALB/c mice were given streptomycin in their drinking water (5 g/L) starting 24 h before colonization. *E. coli* K12 and K12Δ*tnaA* strains were grown to saturation at 37 °C in LB containing streptomycin (100 μg/mL) and were introduced to mice by a single oral gavage (450 μL of culture per mouse, pelleted and resuspended in 200 μL of sterile PBS) at 24 h after initiation of streptomycin treatment. Mice remained on streptomycin for the duration of the experiment. Colonization levels in the gut were indirectly assessed by serial dilution plating of fecal samples on MacConkey agar containing streptomycin (100 μg/mL) and nalidixic acid (50 μg/mL). The resulting colonies were checked for indole production using Kovacs reagent (Sigma-Aldrich) following overnight growth in LB at 37 °C.

AB-PAS Staining for Goblet Cell and Mucus Quantitation. A 1-cm piece of colon around the most distal fecal pellet in the colon was excised and fixed in methacarn solution (60% methanol, 30% chloroform, and 10% glacial acetic acid) for 1 wk. Fixed tissue was processed by two washes each of methanol, 100% ethanol, and xylene substitute for 30 min, 20 min, and 15 min, respectively. The tissue was transferred to the Winship Research Pathology Core Lab at Emory University for paraffin embedding, sectioning, and staining with AB-PAS. Goblet cells were quantified by counting the positive cells per crypt in 20 crypts per section, two sections per mouse. Special care was taken to ensure that only full crypts were counted, in which the base of the crypt and cells up to the lumen were visible and linear. For mucus thickness measurements, 10 measurements per section were taken in two sections per mouse. Microscopy was performed using a Nikon Eclipse 50i with NIS Elements D Software for imaging and crypt measurements.

Detection of Muc2 Immunofluorescence. Slides of methacarn-fixed tissue were dewaxed by incubation on a slide warmer at 60 °C for 10 min, followed by two 10-min incubations in xylene substitute (CitriSolv). Sections were rehydrated in decreasing concentrations of ethanol (100%, 95%, 70%, 50%, and 30%) for 5 min each. Antigen retrieval was performed by microwaving slides in antigen retrieval solution (10 mM citric acid, pH 6.0) for 5 min at 300 W thrice and then left at room temperature for 30 min. Slides were blocked (5% FBS in PBS) for 30 min at room temperature and then incubated with anti-Muc2 (1:200 in blocking solution) overnight at 4 °C. Slides were washed with PBS thrice for 10 min each, followed by application of anti-rabbit FITC secondary antibody (The Jackson Laboratory; 1:100) for 2 h at room temperature. Finally, DAPI (1:1,000) was applied for 5 min, followed by three 10-min washes in PBS and mounting in Vectashield.

Detection of Ki67, pHH3(Ser10), and CgA by Immunofluorescence. Distal colon tissue was excised and fixed in 4% paraformaldehyde for 24 h before processing, embedding, and sectioning by the Winship Research Pathology Core Lab at Emory University. Slides were dewaxed by incubation on a slide warmer at 60 °C for 10 min, followed by two 10-min incubations in xylene substitute (CitriSolv). Sections were rehydrated in decreasing concentrations of ethanol (100%, 95%, 70%, 50%, and 30%) for 5 min each. Antigen retrieval was performed by microwaving slides in antigen retrieval solution (10 mM citric acid, pH 6.0) for 5 min at 300 W thrice and then left at room temperature for 30 min. Slides were permeabilized in 0.1% Triton-X in PBS for 5 min and then blocked (0.1% Triton-X and 10% donkey serum in PBS) for 1 h at room temperature. Primary antibody (Ki67, 1:500; pHH3, 1:1,000, CgA, 1:400) in blocking solution was applied overnight at 4 °C in a humid chamber. Slides were washed three times for 15 min each in 0.1% PBS-T, followed by incubation with anti-rabbit Cy3 secondary antibody (The Jackson Laboratory; 1:100) in a dark humid chamber for 2 h at room temperature and DAPI (1:1,000) for 5 min. Finally, slides were washed three times for 15 min each in PBS-T and mounted in Vectashield. Positive cells were counted in 20 sections per crypt.

Fluorescence Microscopy. Immunofluorescent images were acquired with a scientific-grade cooled charge-coupled device (Cool-Snap HQ with ORCA-ER chip) on a multiwavelength, wide-field 3D microscopy system (Intelligent Imaging Innovations), based on a 200 M inverted Zeiss microscope using a 20× lens with a numerical aperture of 0.5 lens. Immunofluorescent samples were imaged at room temperature using a standard Sedat filter set (Chroma Technology).

Detection of IL-22 by ELISA. Here 2-cm segments of distal colons and terminal ileum were excised, washed in HBSS supplemented with penicillin and streptomycin, and cut into 1-cm segments. These segments were cultured for 24 h in 24-well flat-bottom culture plates in RPMI 1640 medium supplemented with penicillin and streptomycin. Supernatant was collected and centrifuged at 5,000 × *g* for 10 min at 4 °C. The concentration of IL-22 was measured using an ELISA kit (Invitrogen).

RNA Sample Preparation and qPCR for Detection of *Il10* Transcript. Here 1-cm segments of transverse colon were excised and placed directly in TRI reagent (Ambion) on ice. Tissue was homogenized in Bullet Blender Green Eppendorf lysis tubes using a Bullet Blender Storm following the manufacturer's protocol for intestinal samples. RNA was extracted using the TRI reagent manufacturer's protocol. Reverse transcription was performed using the RevertAid First-Strand cDNA Synthesis Kit (Thermo Fisher Scientific) with the oligo(dT)18 primer. qPCR was performed using iQ SYBR Green Supermix with a MyiQ real-time PCR system (Bio-Rad). The ΔΔCT method was used to quantify relative gene expression compared with *Gapdh* and *B-actin* controls, using following primers: *Gapdh* forward, 5′ AGG TCG GTG TGA ACG GAT TTG 3′; *Gapdh* reverse, 5′ TGT AGA CCA TGT AGT TGA GGT CA 3′; *B-actin* forward, 5′ GGC TGT ATT CCC CTC CAT CG 3′; *B-actin* reverse, CCA

GTT GGT AAC AAT GCC ATG T 3′; mouse *Il-10* forward, 5′ GCT CTT ACT GAC TGG CAT GAG 3′; mouse *Il-10* reverse, 5′ CGC AGC TCT AGG AGC ATG TG 3′. The data generated by qPCR assays were normalized using the average value of the vehicle treatment control group.

Statistical Analysis. Significance was assessed using GraphPad Prism 7 software. Comparisons were made using the Mann–Whitney *U* test, Kruskal–Wallace analysis of variance (ANOVA) with Dunn's multiple comparison test, or two-way ANOVA. Nonparametric tests were appropriate for most of the processes under study here, because the distribution of the data remains unknown. Rank-sum tests calculate exact probabilities for the null hypothesis, and we report the probability of obtaining the observed distribution of ranked data by chance. Thus, $P = 0.01$ or $P = 0.15$ means that the observed ranking of values would be observed only 1 time or 15 times, respectively, in 100 repeats of the experiment. In most cases, the signal-to-noise ratio is high enough to keep the value well below the 0.05 convention for significance; however, with variant data, interpretation of significance and import is based on the sample size, the meaningful effect size, and other considerations, such as relevant previous evidence, plausibility of the mechanism, number of repeats, uncertainty, and variation in effect size.

Data Availability. All pertinent data are presented in the main text.

ACKNOWLEDGMENTS. We thank Debalina Chaudhuri for reviewing the manuscript and Tesia Cleverley for helpful discussions. This work was supported by NIH Grants 2R01DK074731-04A1 and 5R21AG054903-02.

1. R. An *et al*., Age-dependent changes in GI physiology and microbiota: Time to reconsider? *Gut* **67**, 2213–2222 (2018).
2. S. Kim, S. M. Jazwinski, The gut microbiota and healthy aging: A mini-review. *Gerontology* **64**, 513–520 (2018).
3. N. Thevaranjan *et al*., Age-associated microbial dysbiosis promotes intestinal permeability, systemic inflammation, and macrophage dysfunction. *Cell Host Microbe* **21**, 455–466.e4 (2017).
4. A. Biragyn, L. Ferrucci, Gut dysbiosis: A potential link between increased cancer risk in ageing and inflammaging. *Lancet Oncol.* **19**, e295–e304 (2018).
5. R. Okumura, K. Takeda, Roles of intestinal epithelial cells in the maintenance of gut homeostasis. *Exp. Mol. Med.* **49**, e338 (2017).
6. J. Beumer, H. Clevers, Regulation and plasticity of intestinal stem cells during homeostasis and regeneration. *Development* **143**, 3639–3649 (2016).
7. C. T. Capaldo, D. N. Powell, D. Kalman, Layered defense: How mucus and tight junctions seal the intestinal barrier. *J. Mol. Med.* **95**, 927–934 (2017).
8. M. E. V. Johansson, Fast renewal of the distal colonic mucus layers by the surface goblet cells as measured by in vivo labeling of mucin glycoproteins. *PLoS One* **7**, e41009 (2012).
9. M. Van der Sluis *et al*., Muc2-deficient mice spontaneously develop colitis, indicating that MUC2 is critical for colonic protection. *Gastroenterology* **131**, 117–129 (2006).
10. M. E. V. Johansson *et al*., The inner of the two Muc2 mucin-dependent mucus layers in colon is devoid of bacteria. *Proc. Natl. Acad. Sci. U.S.A.* **105**, 15064–15069 (2008).
11. K. S. B. Bergstrom *et al*., Muc2 protects against lethal infectious colitis by disassociating pathogenic and commensal bacteria from the colonic mucosa. *PLoS Pathog.* **6**, e1000902 (2010).
12. M. Zarepour *et al*., The mucin Muc2 limits pathogen burdens and epithelial barrier dysfunction during Salmonella enterica serovar Typhimurium colitis. *Infect. Immun.* **81**, 3672–3683 (2013).
13. F. Gerbe *et al*., Intestinal epithelial tuft cells initiate type 2 mucosal immunity to helminth parasites. *Nature* **529**, 226–230 (2016).
14. V. Strugala, P. W. Dettmar, J. P. Pearson, Thickness and continuity of the adherent colonic mucus barrier in active and quiescent ulcerative colitis and Crohn's disease. *Int. J. Clin. Pract.* **62**, 762–769 (2008).
15. T. Zelante *et al*., Tryptophan catabolites from microbiota engage aryl hydrocarbon receptor and balance mucosal reactivity via interleukin-22. *Immunity* **39**, 372–385 (2013).
16. B. Bommarius *et al*., A family of indoles regulate virulence and Shiga toxin production in pathogenic E. coli. *PLoS One* **8**, e54456 (2013).
17. A. Swimm *et al*., Indoles derived from intestinal microbiota act via type I interferon signaling to limit graft-versus-host disease. *Blood* **132**, 2506–2519 (2018).
18. R. Sonowal *et al*., Indoles from commensal bacteria extend healthspan. *Proc. Natl. Acad. Sci. U.S.A.* **114**, E7506–E7515 (2017).
19. J. Qiu *et al*., Group 3 innate lymphoid cells inhibit T-cell-mediated intestinal inflammation through aryl hydrocarbon receptor signaling and regulation of microflora. *Immunity* **39**, 386–399 (2013).
20. J. Qiu *et al*., The aryl hydrocarbon receptor regulates gut immunity through modulation of innate lymphoid cells. *Immunity* **36**, 92–104 (2012).
21. C. A. Lindemans *et al*., Interleukin-22 promotes intestinal stem cell-mediated epithelial regeneration. *Nature* **528**, 560–564 (2015).
22. A. Mizoguchi *et al*., Clinical importance of IL-22 cascade in IBD. *J. Gastroenterol.* **53**, 465–474 (2018).
23. N. Powell *et al*., Interleukin-22 orchestrates a pathological endoplasmic reticulum stress response transcriptional programme in colonic epithelial cells. *Gut* **69**, 578–590 (2020).
24. T. D. Hubbard, I. A. Murray, G. H. Perdew, Indole and tryptophan metabolism: Endogenous and dietary routes to Ah receptor activation. *Drug Metab. Dispos.* **43**, 1522–1535 (2015).
25. R. Kühn, J. Löhler, D. Rennick, K. Rajewsky, W. Müller, Interleukin-10-deficient mice develop chronic enterocolitis. *Cell* **75**, 263–274 (1993).
26. D. S. Shouval *et al*., "Interleukin 10 receptor signaling" in *Advances in Immunology*, F. W. Alt, Ed. (Elsevier, 2014), pp. 177–210.
27. J. W. Collins *et al*., Citrobacter rodentium: Infection, inflammation and the microbiota. *Nat. Rev. Microbiol.* **12**, 612–623 (2014).
28. J.-H. Lee, T. K. Wood, J. Lee, Roles of indole as an interspecies and interkingdom signaling molecule. *Trends Microbiol.* **23**, 707–718 (2015).
29. S. M. Dann *et al*., Attenuation of intestinal inflammation in interleukin-10-deficient mice infected with Citrobacter rodentium. *Infect. Immun.* **82**, 1949–1958 (2014).
30. J.-H. Park, J.-M. Lee, E.-J. Lee, W.-B. Hwang, D.-J. Kim, Indole-3-carbinol promotes goblet cell differentiation regulating Wnt and Notch signaling pathways AhR-dependently. *Mol. Cells* **41**, 290–300 (2018).
31. T. Fülöp, A. Larbi, J. M. Witkowski, Human inflammaging. *Gerontology* **65**, 495–504 (2019).
32. T. Pelaseyed *et al*., The mucus and mucins of the goblet cells and enterocytes provide the first defense line of the gastrointestinal tract and interact with the immune system. *Immunol. Rev.* **260**, 8–20 (2014).
33. B. Sovran *et al*., Age-associated impairment of the mucus barrier function is associated with profound changes in microbiota and immunity. *Sci. Rep.* **9**, 1437 (2019).
34. S. Soenen, C. K. Rayner, K. L. Jones, M. Horowitz, The ageing gastrointestinal tract. *Curr. Opin. Clin. Nutr. Metab. Care* **19**, 12–18 (2016).
35. E. E. Alexeev *et al*., Microbiota-derived indole metabolites promote human and murine intestinal homeostasis through regulation of interleukin-10 receptor. *Am. J. Pathol.* **188**, 1183–1194 (2018).
36. H. Rhinn, A. Abeliovich, Differential aging analysis in human cerebral cortex identifies variants in TMEM106B and GRN that regulate aging phenotypes. *Cell Syst.* **4**, 404–415.e5 (2017).
37. S. S. Khan, B. D. Singer, D. E. Vaughan, Molecular and physiological manifestations and measurement of aging in humans. *Aging Cell* **16**, 624–633 (2017).
38. D. B. Bartlett *et al*., The age-related increase in low-grade systemic inflammation (inflammaging) is not driven by cytomegalovirus infection. *Aging Cell* **11**, 912–915 (2012).
39. D. Rennick, N. Davidson, D. Berg, Interleukin-10 gene knock-out mice: A model of chronic inflammation. *Clin. Immunol. Immunopathol.* **76**, S174–S178 (1995).
40. G. Sikka *et al*., Interleukin 10 knockout frail mice develop cardiac and vascular dysfunction with increased age. *Exp. Gerontol.* **48**, 128–135 (2013).
41. F. Ko *et al*., Inflammation and mortality in a frail mouse model. *Age (Dordr.)* **34**, 705–715 (2012).
42. C. P. Verschoor *et al*., Circulating muramyl dipeptide is negatively associated with interleukin-10 in the frail elderly. *Inflammation* **38**, 272–277 (2015).
43. D. Weber *et al*., Low urinary indoxyl sulfate levels early after transplantation reflect a disrupted microbiome and are associated with poor outcome. *Blood* **126**, 1723–1728 (2015).
44. National Research Council, *Guide for the Care and Use of Laboratory Animals*, (National Academies Press, ed. 8, 2011).